SUPPORTING INFORMATION AVAILABLE

Inferring the anthropogenic NO_x emission trend over the United States during 2003 - 2017 from satellite observations: Was there a flattening of the emission trend after the Great Recession?

Jianfeng Li[1, a], Yuhang Wang[1*]

[1]School of Earth and Atmospheric Sciences, Georgia Institute of Technology, Atlanta, Georgia, USA

[a] Now at Pacific Northwest National Laboratory, Richland, WA, USA

[*] *Correspondence to* Yuhang Wang (yuhang.wang@eas.gatech.edu)

Figure Captions

Figure S1. Annual variation of NO_3^- wet deposition fluxes for each season from 2003 – 2017. The fluxes were scaled by the corresponding values in 2003. Shaded regions denote standard deviations. Monthly NO_3^- wet deposition observations are obtained from https://nadp.slh.wisc.edu/data/NTN/ntnAllsites.aspx (last access, September 29, 2019).

Figure S2. Comparison between original EPA anthropogenic NO_x emissions and updated EPA anthropogenic NO_x emissions with the newest Continuous Emission Monitoring Systems (CEMS) measurements.

Figure S3. Daily OMI NO_2 TVCDs for July 2011 (a) and 2012 (b) in Atlanta (33.755° N, 84.39° W). Black circles are weekday values, and red circles are weekend values. We find significant daily variations of NO_2 TVCD from (a) and (b). The number of available measurements in July 2011 is much less than July 2012. We find clear larger NO_2 TVCD values on weekdays than on weekends in July 2011, but the difference between weekday and weekday TVCDs in July 2012 are not so obvious.

Figure S4. Hourly averaged ratios of FEM (a) and CAPS (b) to FRM NO_2 measurements in each season, respectively. The FEM/FRM ratios are computed from coincident FRM and FEM measurements from 2013 – 2015 at 4 sites. The CAPS/FRM ratios are calculated based on coincident CAPS and FRM data from 2015 – 2016 at 3 sites.

Figure S5. Annual variations of AQS NO_2 surface concentrations at different hours on weekdays in spring (a, b), summer (c, d), autumn (e, f), and winter (g, h). Left panels show absolute NO_2 concentrations, and right panels are their relative variations normalized to 2011. To conduct reliable and consistent comparisons, we only used monitoring sites satisfying the seasonal *RCI* < 50% and continuity criteria on weekdays from 2003 – 2017.

Figure S6. Distributions of (a) NO_2 TVCD fraction that is in the boundary layer (< 2810 m) at 13:00 – 14:00, (b) NO_2 TVCD fraction in the boundary layer (< 1290 m) at 10:00 – 11:00, (c) the fraction of soil NO_x emissions in all surface sources (anthropogenic + soil) on weekdays for July 2011. As the lifetime of NO_2 in the free troposphere (several days ~ 2 weeks) is much longer than that in the boundary layer (~ 10 hours), local lightning NO_x emissions cannot represent NO_2 VCDs in the free troposphere. In this study, we apply NO_2 VCD in the free troposphere to analyze the impact of lighting NO_x on the nonlinear relationships between anthropogenic NO_x emissions and NO_2 TVCDs and use lightning NO_x and NO_2 VCD in the free troposphere interchangeably in the following.

Figure S7. (a) Distributions of the fractions of surface NO_x emissions emitted by soil ("SoilNO_x"), the portions of NO_2 TVCDs in the boundary layer ("PBLVCD"), and the fractions of NO_2 TVCDs from anthropogenic NO_x emissions ("AnthroVCD") as functions of NEI2011 anthropogenic NO_x emissions at 13:00 – 14:00 LT on weekdays for July 2011 over the CONUS. The fraction of NO_2 TVCDs from anthropogenic NO_x emissions is equal to $\left(1-\frac{E_{soil}}{E_{soil}+E_{anthropogenic}}\right)\times\left(\frac{TVCD_{boundary}}{TVCD_{boundary}+TVCD_{free}}\right)$, where E_{soil} denotes soil NO_x emissions, $E_{anthropogenic}$ denotes anthropogenic NO_x emissions, $TVCD_{boundary}$ denotes NO_2 TVCDs in the boundary layer, and $TVCD_{free}$ denotes NO_2 TVCDs in the free troposphere. The calculated data are grouped into 9 bins as in Figure 2. (b) Same as (a), but for 10:00 – 11:00 LT. (c) Distributions of β_{Emis}, γ_{Emis}, β, and γ as functions of anthropogenic NO_x emissions at 13:00 – 14:00 LT on weekdays for July 2011 over the CONUS. β and γ are the same as Figure 2. β_{Emis} and γ_{Emis} denote β and γ values when no other factors are taken into consideration except for soil NO_x emissions, anthropogenic NO_x emissions, and NO_2 in the free troposphere. $\beta_{Emis}=\frac{15\%}{15\%\times\left(\frac{E_{anthropogenic}}{E_{anthropogenic}+E_{soil}}\right)\left(\frac{TVCD_{boundary}}{TVCD_{boudnary}+TVCD_{free}}\right)}=\left(\frac{E_{anthropogenic}+E_{soil}}{E_{anthropogenic}}\right)\left(\frac{TVCD_{boundary}+TVCD_{free}}{TVCD_{boundary}}\right)$,

and $\gamma_{Emis} = \frac{15\%}{15\% \times \left(\frac{E_{anthropogenic}}{E_{anthropogenic}+E_{soil}}\right)} = \left(\frac{E_{anthropogenic}+E_{soil}}{E_{anthropogenic}}\right)$. It is noteworthy that here we assume no interactions between the boundary layer and the free troposphere, boundary-layer NO_x are only related to soil and anthropogenic NO_x emissions, and lightning NO_x only affect NO_2 in the free troposphere. The assumptions are reasonable as the time scale (~ 1 week) of the interactions between the boundary layer and the free troposphere is much longer than NO_x lifetime in the boundary layer, and only a small fraction of lightning NO_x is distributed into the boundary layer in this study. Therefore, β_{Emis} and γ_{Emis} roughly represent the contributions of background sources (lightning NO_x and soil NO_x) to β and γ values. The differences between β (γ) and β_{Emis} (γ_{Emis}) indicate the contribution of non-emission factors to β (γ) values, such as chemistry, transport, NO_2 hydrolysis on aerosols, and dry deposition. (d) Same as (c), but for 10:00 – 11:00 LT. From (c) and (d), we find that both background sources (lightning NO_x + soil NO_x) and non-emission factors are important when considering the nonlinear relationships among NO_x emissions, NO_2 surface concentrations, and NO_2 TVCDs in low-anthropogenic-NO_x emission regions. (e) Distribution of NO_x chemical lifetimes as functions of anthropogenic NO_x emissions at 11:00 – 14:00 LT on weekdays for July 2011 over the CONUS. "Standard_surf" denotes NO_x chemical lifetimes at the surface layer from the standard REAM simulation ("group 1" in Section 3.1); "Standard_trop" denotes average NO_x chemical lifetimes in the troposphere for "group 1"; "Reduce_surf" denotes NO_x chemical lifetimes at the surface layer for "group 2" with anthropogenic NO_x emissions reduced by 15%; "Reduce_trop" denotes average NO_x chemical lifetimes in the troposphere for "group 2". In this study, we used the lifetimes at 11:00 – 14:00 LT but not 13:00 – 14:00 LT to partly include the accumulation effect of NO_x emissions: NO_2 TVCD and NO_2 surface concentrations at 13:00 – 14:00 LT are not only affected by NO_x emissions at 13:00 – 14:00 LT but also by NO_x emissions before that due to the NO_x chemical lifetime of several hours in daytime. (f) Same as (e), but for 8:00 – 11:00 LT. (g) Relative changes of NO_x chemical lifetimes at 11:00 – 14:00 LT on weekdays for July 2011 over the

CONUS due to the 15% decrease of anthropogenic NO_x emissions in "group 2". "Surface" denotes the relative changes of NO_x chemical lifetimes at the surface, while "Troposphere" denotes the relative changes of average NO_x chemical lifetimes in the troposphere. We first calculated the relative changes in each grid cell via $\frac{lifetime_{Reduce}}{lifetime_{Standard}} - 1$, and then binned the calculated data into 9 groups as Figure 2. (h) Same as (g), but for 8:00 – 11:00 LT. In the chemical lifetime calculation, we included sinks from the reaction of OH + NO_2 and net losses due to organic nitrate production from the reactions of RO_2 with NO or NO_2 except for peroxyacyl nitrates (PANs), because PANs can be either a source or sink of NO_x depending on transport and chemistry. Only accounting for the sink from the reaction of OH + NO_2 produces significant different lifetimes in low-anthropogenic-NO_x emission bins and has less impact on high-anthropogenic-NO_x emission regions, which, however, does not affect our conclusions derived from subpanels (g) and (h) (the mean relative differences of chemical lifetimes between "group 1" and "group 2" are still < 10% in all bins): the chemical nonlinearity contributes little to β and γ values in low-anthropogenic-NO_x emission regions. Although not shown here, the impacts of NO_2 hydrolysis and NO_2 dry deposition on β and γ values are even smaller than those of chemical nonlinearity. Therefore, the differences between β (γ) and β_{Emis} (γ_{Emis}) in low-anthropogenic-NO_x emission bins in (c) and (d) mainly indicate the contribution of transport to β (γ) values. Error bars in (a), (b), (g), and (h) denote standard deviations.

Figure S8. Same as Figure 4, but for AQS NO_2 surface concentrations and coincident GOME-2A NO_2 TVCD data during 2008 – 2016.

Figure S9. Relative variations of OMI-QA4ECV NO_2 TVCD data for urban regions (black lines) and the whole CONUS (red lines) from 2005 – 2017 in 4 seasons.

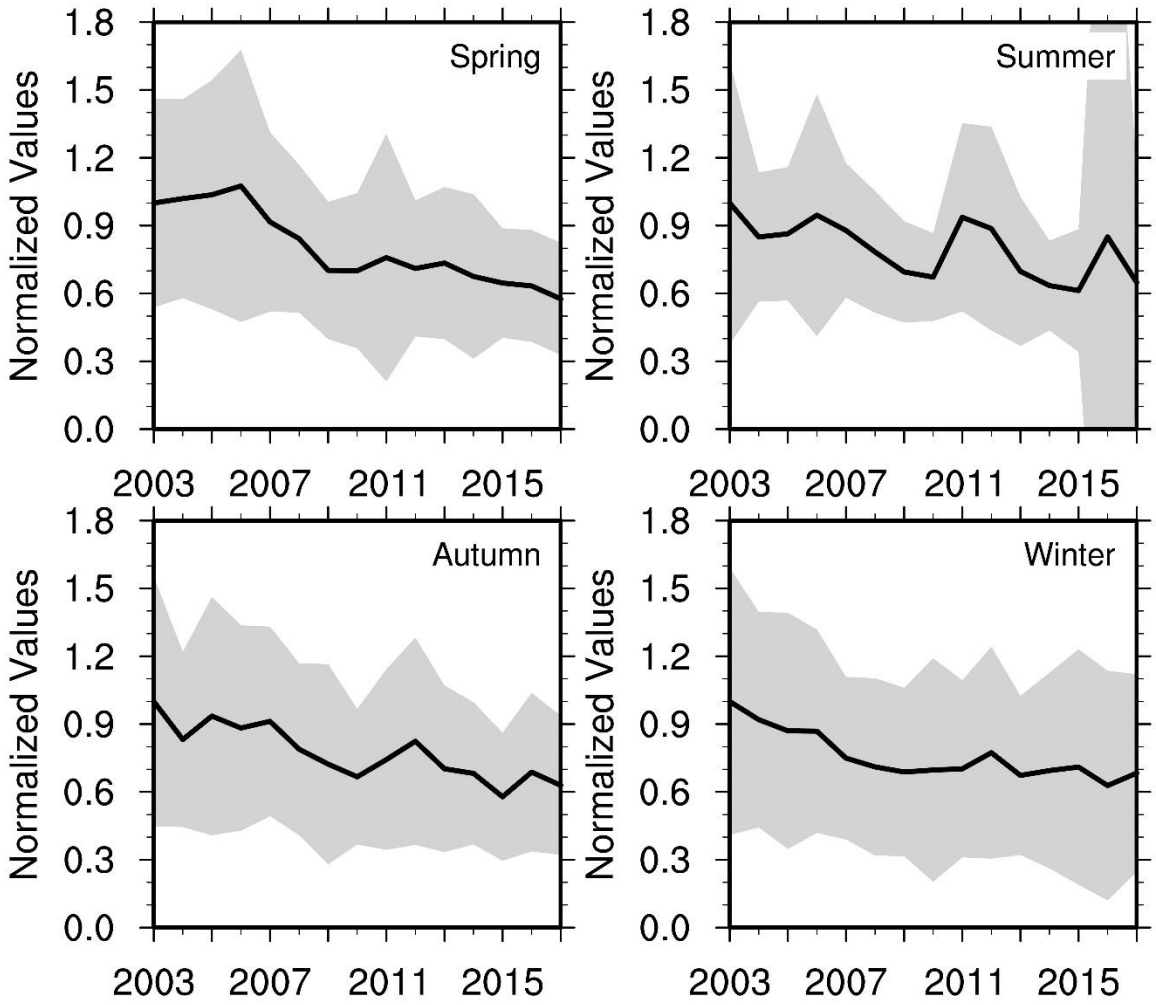

107

108 Figure S1. Annual variation of NO_3^- wet deposition fluxes for each season from 2003 – 2017. The
109 fluxes were scaled by the corresponding values in 2003. Shaded regions denote standard
110 deviations. Monthly NO_3^- wet deposition observations are obtained from
111 https://nadp.slh.wisc.edu/data/NTN/ntnAllsites.aspx (last access, September 29, 2019).

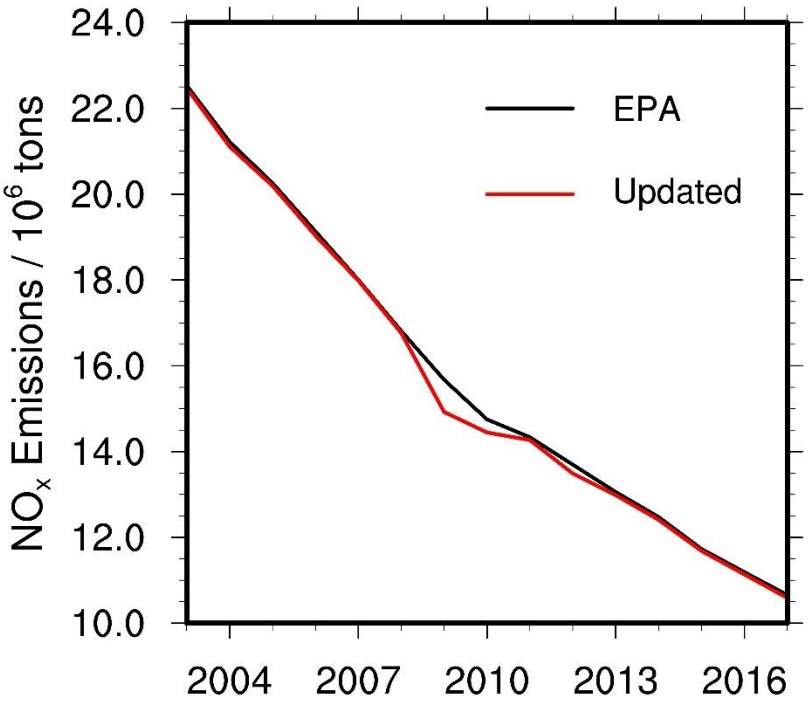

112

113 Figure S2. Comparison between original EPA anthropogenic NO_x emissions and updated EPA

114 anthropogenic NO_x emissions with the newest Continuous Emission Monitoring Systems

115 (CEMS) measurements.

116

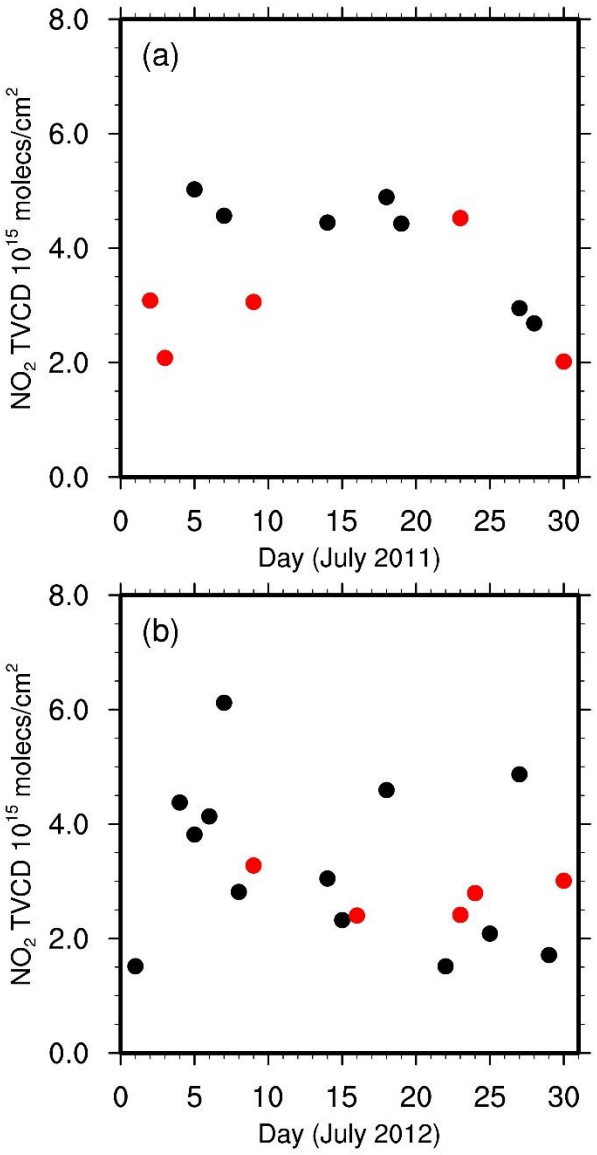

117

118 Figure S3. Daily OMI NO_2 TVCDs for July 2011 (a) and 2012 (b) in Atlanta (33.755° N, 84.39°
119 W). Black circles are weekday values, and red circles are weekend values. We find significant
120 daily variations of NO_2 TVCD from (a) and (b). The number of available measurements in July
121 2011 is much less than July 2012. We find clear larger NO_2 TVCD values on weekdays than on
122 weekends in July 2011, but the difference between weekday and weekday TVCDs in July 2012
123 are not so obvious.

124

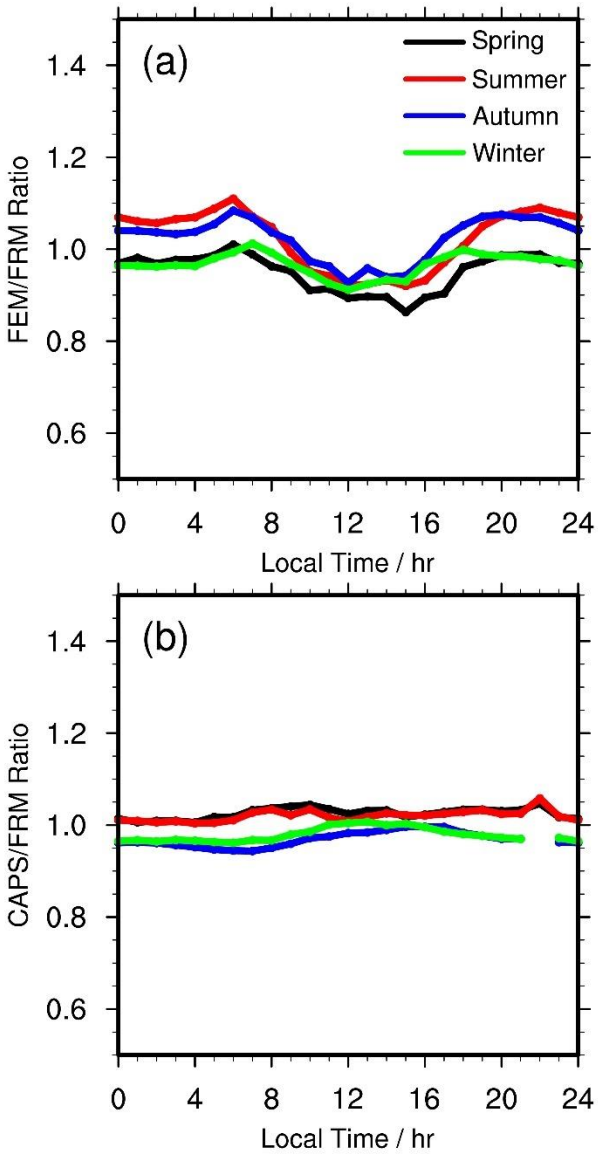

125

126 Figure S4. Hourly averaged ratios of FEM (a) and CAPS (b) to FRM NO_2 measurements in each
127 season, respectively. The FEM/FRM ratios are computed from coincident FRM and FEM
128 measurements from 2013 – 2015 at 4 sites. The CAPS/FRM ratios are calculated based on
129 coincident CAPS and FRM data from 2015 – 2016 at 3 sites.

130

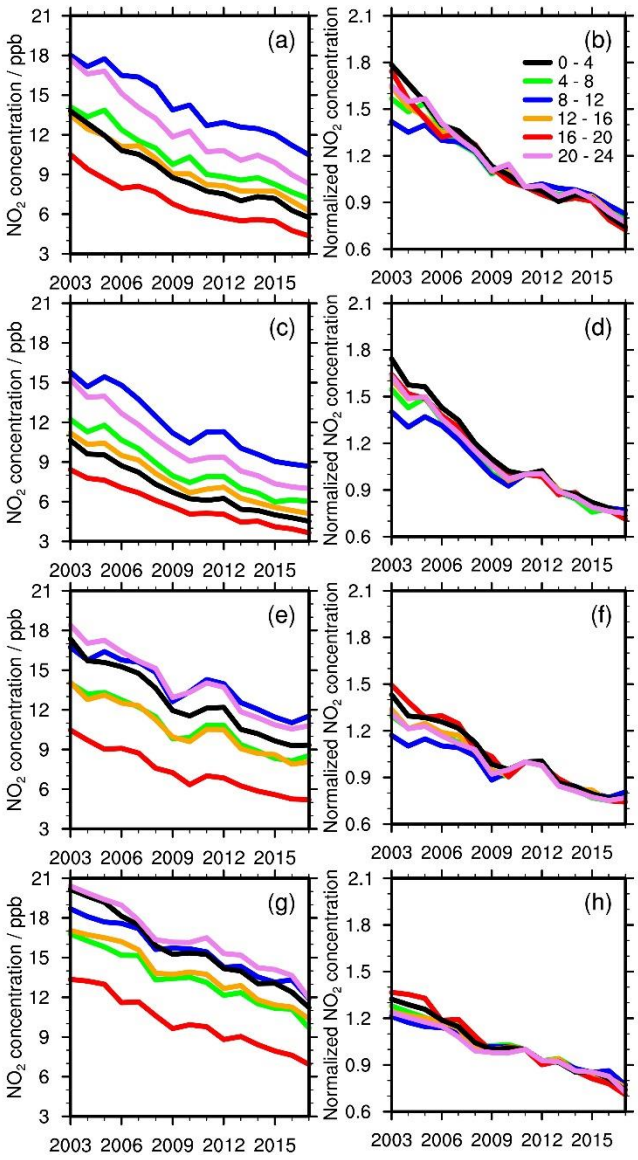

131

132 Figure S5. Annual variations of AQS NO_2 surface concentrations at different hours on weekdays
133 in spring (a, b), summer (c, d), autumn (e, f), and winter (g, h). Left panels show absolute NO_2
134 concentrations, and right panels are their relative variations normalized to 2011. To conduct
135 reliable and consistent comparisons, we only used monitoring sites satisfying the seasonal *RCI* <
136 50% and continuity criteria on weekdays from 2003 – 2017.

137

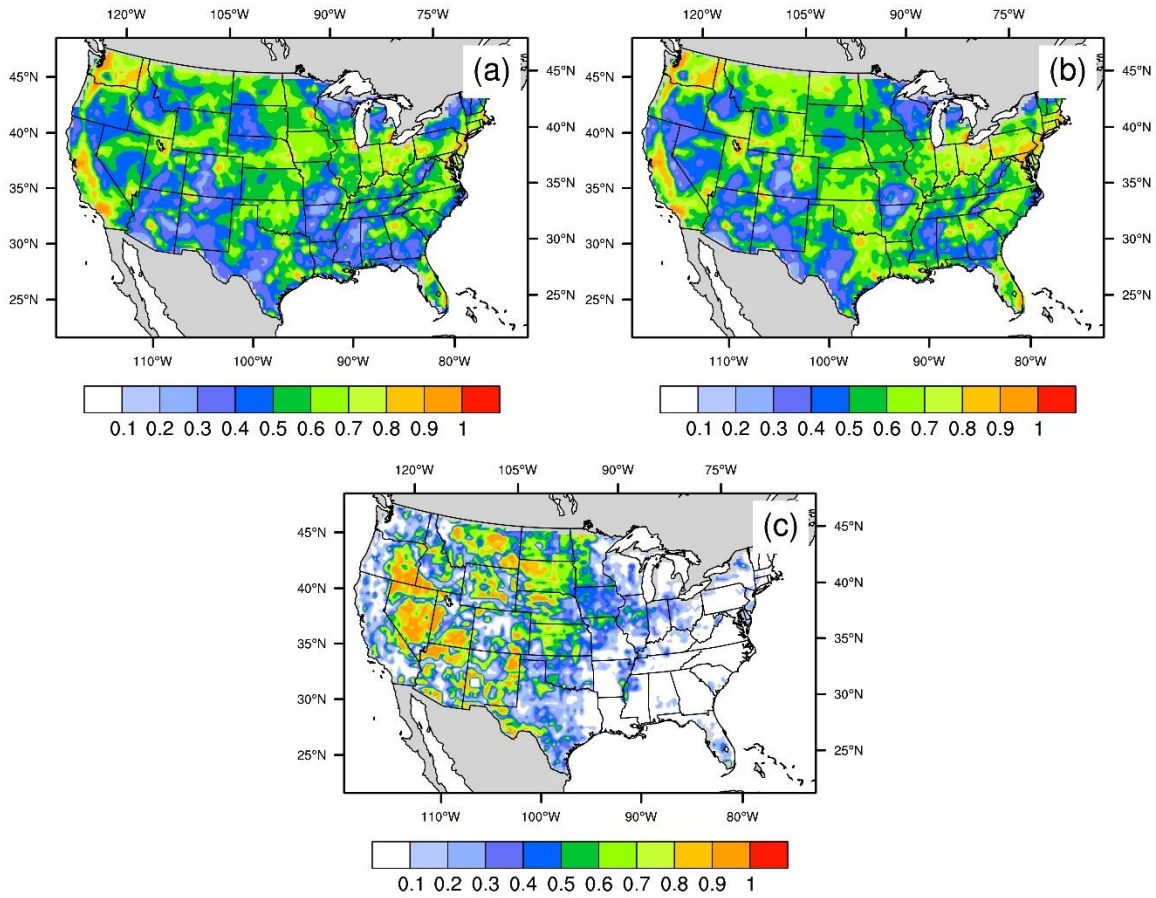

Figure S6. Distributions of (a) NO_2 TVCD fraction that is in the boundary layer (< 2810 m) at 13:00 – 14:00, (b) NO_2 TVCD fraction in the boundary layer (< 1290 m) at 10:00 – 11:00, (c) the fraction of soil NO_x emissions in all surface sources (anthropogenic + soil) on weekdays for July 2011. As the lifetime of NO_2 in the free troposphere (several days ~ 2 weeks) is much longer than that in the boundary layer (~ 10 hours), local lightning NO_x emissions cannot represent NO_2 VCDs in the free troposphere. In this study, we apply NO_2 VCD in the free troposphere to analyze the impact of lighting NO_x on the nonlinear relationships between anthropogenic NO_x emissions and NO_2 TVCDs and use lightning NO_x and NO_2 VCD in the free troposphere interchangeably in the following.

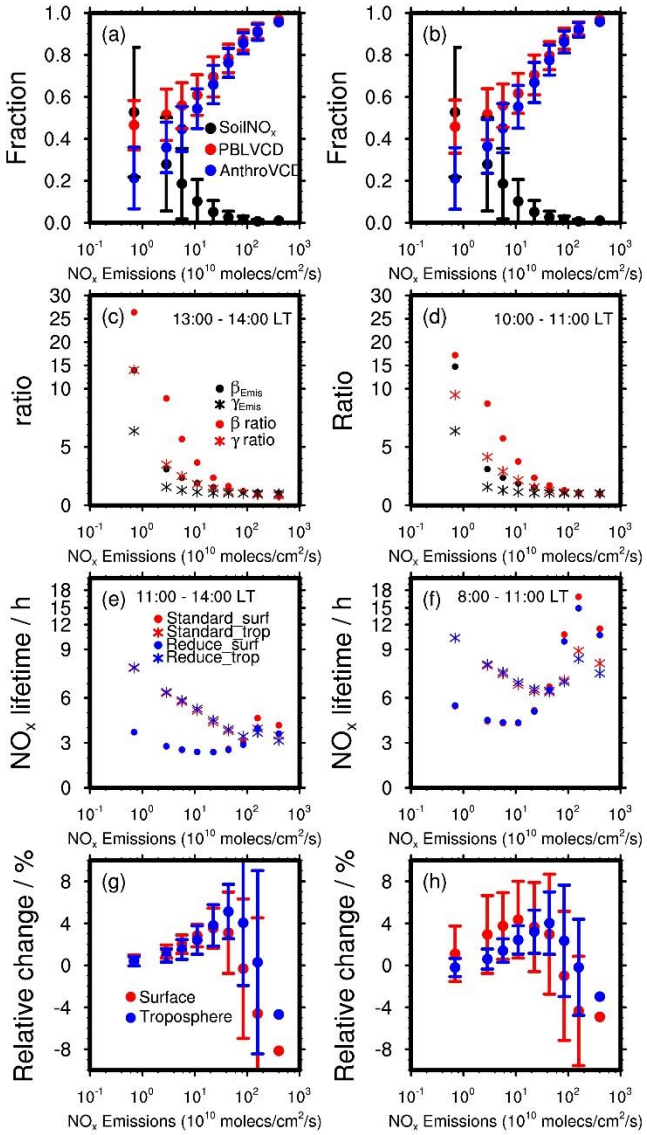

Figure S7. (a) Distributions of the fractions of surface NO_x emissions emitted by soil ("SoilNO_x"), the portions of NO_2 TVCDs in the boundary layer ("PBLVCD"), and the fractions of NO_2 TVCDs from anthropogenic NO_x emissions ("AnthroVCD") as functions of NEI2011 anthropogenic NO_x emissions at 13:00 – 14:00 LT on weekdays for July 2011 over the CONUS. The fraction of NO_2 TVCDs from anthropogenic NO_x emissions is equal to $\left(1 -\right.$

$\frac{E_{soil}}{E_{soil}+E_{anthropogenic}}\Big) \times \Big(\frac{TVCD_{boundary}}{TVCD_{boundary}+TVCD_{free}}\Big)$, where E_{soil} denotes soil NO_x emissions, $E_{anthropogenic}$ denotes anthropogenic NO_x emissions, $TVCD_{boundary}$ denotes NO_2 TVCDs in the boundary layer, and $TVCD_{free}$ denotes NO_2 TVCDs in the free troposphere. The calculated data are grouped into 9 bins as in Figure 2. (b) Same as (a), but for 10:00 – 11:00 LT. (c) Distributions of β_{Emis}, γ_{Emis}, β, and γ as functions of anthropogenic NO_x emissions at 13:00 – 14:00 LT on weekdays for July 2011 over the CONUS. β and γ are the same as Figure 2. β_{Emis} and γ_{Emis} denote β and γ values when no other factors are taken into consideration except for soil NO_x emissions, anthropogenic NO_x emissions, and NO_2 in the free troposphere. $\beta_{Emis} = \frac{15\%}{15\%\times\left(\frac{E_{anthropogenic}}{E_{anthropogenic}+E_{soil}}\right)\left(\frac{TVCD_{boundary}}{TVCD_{boudnary}+TVCD_{free}}\right)} = \left(\frac{E_{anthropogenic}+E_{soil}}{E_{anthropogenic}}\right)\left(\frac{TVCD_{boundary}+TVCD_{free}}{TVCD_{boundary}}\right)$, and $\gamma_{Emis} = \frac{15\%}{15\%\times\left(\frac{E_{anthropogenic}}{E_{anthropogenic}+E_{soil}}\right)} = \left(\frac{E_{anthropogenic}+E_{soil}}{E_{anthropogenic}}\right)$. It is noteworthy that here we assume no interactions between the boundary layer and the free troposphere, boundary-layer NO_x are only related to soil and anthropogenic NO_x emissions, and lightning NO_x only affect NO_2 in the free troposphere. The assumptions are reasonable as the time scale (~ 1 week) of the interactions between the boundary layer and the free troposphere is much longer than NO_x lifetime in the boundary layer, and only a small fraction of lightning NO_x is distributed into the boundary layer in this study. Therefore, β_{Emis} and γ_{Emis} roughly represent the contributions of background sources (lightning NO_x and soil NO_x) to β and γ values. The differences between β (γ) and β_{Emis} (γ_{Emis}) indicate the contribution of non-emission factors to β (γ) values, such as chemistry, transport, NO_2 hydrolysis on aerosols, and dry deposition. (d) Same as (c), but for 10:00 – 11:00 LT. From (c) and (d), we find that both background sources (lightning NO_x + soil NO_x) and non-emission factors are important when considering the nonlinear relationships among NO_x emissions, NO_2 surface concentrations, and NO_2 TVCDs in low-anthropogenic-NO_x emission regions. (e) Distribution of NO_x chemical lifetimes as functions of anthropogenic NO_x

emissions at 11:00 – 14:00 LT on weekdays for July 2011 over the CONUS. "Standard_surf" denotes NO_x chemical lifetimes at the surface layer from the standard REAM simulation ("group 1" in Section 3.1); "Standard_trop" denotes average NO_x chemical lifetimes in the troposphere for "group 1"; "Reduce_surf" denotes NO_x chemical lifetimes at the surface layer for "group 2" with anthropogenic NO_x emissions reduced by 15%; "Reduce_trop" denotes average NO_x chemical lifetimes in the troposphere for "group 2". In this study, we used the lifetimes at 11:00 – 14:00 LT but not 13:00 – 14:00 LT to partly include the accumulation effect of NO_x emissions: NO_2 TVCD and NO_2 surface concentrations at 13:00 – 14:00 LT are not only affected by NO_x emissions at 13:00 – 14:00 LT but also by NO_x emissions before that due to the NO_x chemical lifetime of several hours in daytime. (f) Same as (e), but for 8:00 – 11:00 LT. (g) Relative changes of NO_x chemical lifetimes at 11:00 – 14:00 LT on weekdays for July 2011 over the CONUS due to the 15% decrease of anthropogenic NO_x emissions in "group 2". "Surface" denotes the relative changes of NO_x chemical lifetimes at the surface, while "Troposphere" denotes the relative changes of average NO_x chemical lifetimes in the troposphere. We first calculated the relative changes in each grid cell via $\frac{lifetime_{Reduce}}{lifetime_{Standard}} - 1$, and then binned the calculated data into 9 groups as Figure 2. (h) Same as (g), but for 8:00 – 11:00 LT. In the chemical lifetime calculation, we included sinks from the reaction of OH + NO_2 and net losses due to organic nitrate production from the reactions of RO_2 with NO or NO_2 except for peroxyacyl nitrates (PANs), because PANs can be either a source or sink of NO_x depending on transport and chemistry. Only accounting for the sink from the reaction of OH + NO_2 produces significant different lifetimes in low-anthropogenic-NO_x emission bins and has less impact on high-anthropogenic-NO_x emission regions, which, however, does not affect our conclusions derived from subpanels (g) and (h) (the mean relative differences of chemical lifetimes between "group 1" and "group 2" are still < 10% in all bins): the chemical nonlinearity contributes little to β and γ values in low-anthropogenic-NO_x emission regions. Although not shown here, the

impacts of NO_2 hydrolysis and NO_2 dry deposition on β and γ values are even smaller than those of chemical nonlinearity. Therefore, the differences between β (γ) and β_{Emis} (γ_{Emis}) in low-anthropogenic-NO_x emission bins in (c) and (d) mainly indicate the contribution of transport to β (γ) values. Error bars in (a), (b), (g), and (h) denote standard deviations.

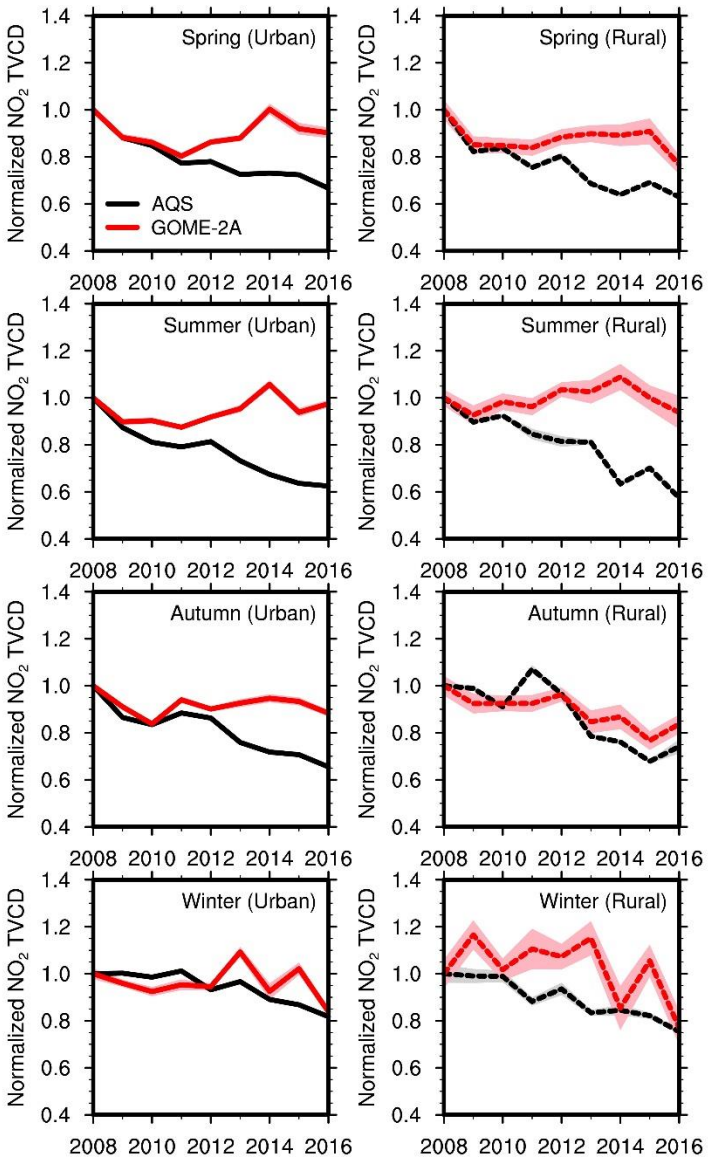

209

210 Figure S8. Same as Figure 4, but for AQS NO_2 surface concentrations and coincident GOME-2A

211 NO_2 TVCD data during 2008 – 2016.

212

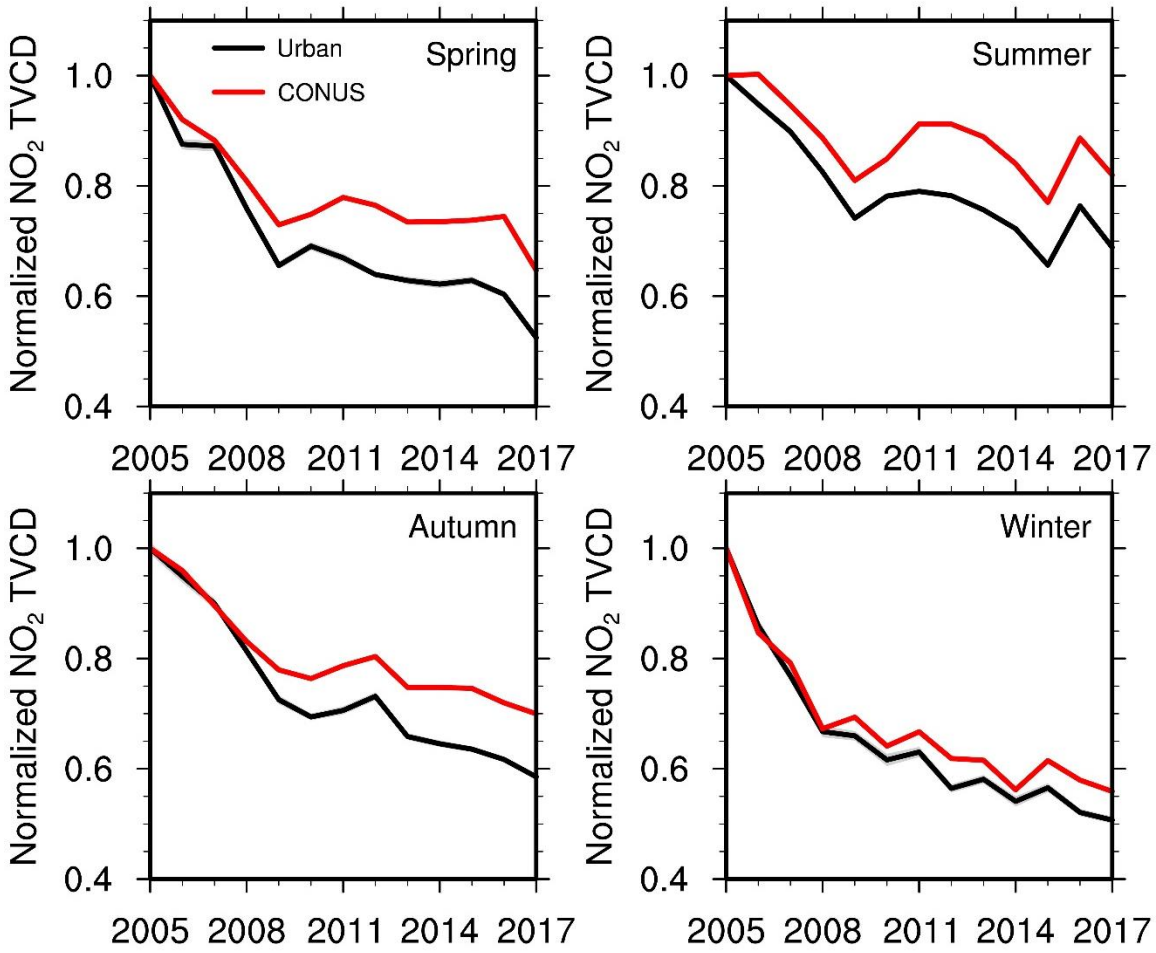

213

214 Figure S9. Relative variations of OMI-QA4ECV NO_2 TVCD data for urban regions (black lines)
215 and the whole CONUS (red lines) from 2005 – 2017 in 4 seasons.

216